Optical and Infrared Modeling

Abdelaziz Kallel
Tartu Observatory
Estonia

1. Introduction

In order to understand the relationships between the vegetation features (namely amount and structure) and the amount of sunlight reflected in the visible and near- to middle-infrared spectral domains many empirical methods based on various vegetation indices (e.g., NDVI, EVI) (Kallel et al., 2007), and physical approach namely based on radiative transfer (RT) theory have been developed. In RT, two model types can be distinguished: (i) one-Dimensional (1-D) models providing a (semi)analytical expression of the Bidirectional Reflectance Distribution Function (BRDF) of canopy architecture, its scattering parameters, and scene geometry (Gobron et al., 1997; Verhoef, 1984; 1998); (ii) 3-D models based on Monte Carlo simulations of a large number of photons randomly propagating through a canopy (Gastellu-Etchegorry et al., 1996; Lewis, 1999; North, 1996). Compared to 1-D models, such 3-D methods allow to take into account canopy heterogeneity with high accuracy. However, they suffer from long running times making their inversion difficult.

The RT theory was first proposed by Chandrasekhar (1950) to study radiation scattering in conventional (i.e. rotationally invariant) media. Such an assumption could be sufficient to model, for example, light scattering in the atmosphere, but appears rudimentary for modeling the reflectance of leaves, or shoots, in a vegetation canopy. To extend the formulation to such a case, many models are proposed. Among the 1-D model, one can cite SAIL (Verhoef, 1984) that is among the most widely used in case of turbid (null size components) crops canopies. The SAIL model allows to derive a non-isotropic BRDF considering two diffuse fluxes (upward/downward flux) to model the multiple scattering of the radiant flux by the vegetation elements. These fluxes are assumed to be semi-isotropic, which is only an approximation that lead to reflectance underestimation (Pinty et al., 2004). As a solution, Verhoef (1998) developed SAIL++ which is a 1-D model providing accurate reflectance estimation in the turbid case. Indeed, this model divides the diffuses fluxes into 72-subfluxes, and turns the SAIL equation system into a matrix-vector equation. Compared to 3-D models of RAMI 2 database in the turbid case (Pinty et al., 2004), SAIL++ gives accurate results.

Another solution to overcome the semi-isotropy assumption in the turbid case will be presented in this chapter, it is based on the coupling between SAIL and Adding method (Cooper et al., 1982; Van de Hulst, 1980). For such a method, optical characteristics of canopy layers such that reflectance and transmittance are directly defined and handled at the scale of the vegetation layer (as operators). Their physical interpretation is hence easier. However, the vegetation description is rather simplistic and the canopy internal geometry is represented with low accuracy. Indeed, in order to retrieve the adding operators for each layer, Cooper et al. (1982) did not take into account the high order interactions between light and vegetation

which are very important as shown in (Pinty et al., 2004). In order to adapt the Adding method to such a configuration, we need a more accurate estimation of the Adding scattering parameters. Since the Adding method operators are derived from the bidirectional reflectance and transmittance of the considered layer, in this study we propose to introduce the SAIL canopy description into the Adding formulation. The developed model is called AddingS.

Now, since the size of vegetation elements cannot be assumed null. Among others, Kuusk (1985) proposed a correction allowing the extension of the RT models like SAIL and SAIL++ to the discrete case (non-null-size components) (Verhoef, 1998). This approach allows to take into account the hot spot effect representing the bright area in the direction opposite to the direction of a pointlike the light source. This effect is caused by the high probability of backscattering which is proportional to the mean size of medium elements. Such an approach suffers from a severe shortcoming: compared to the turbid case, it increases only the reflectance created by the first collision of the radiation by leaves. As this increasing is not followed by the decreasing of other fluxes, it leads to a violation of the energy conservation law (Kallel, 2007). Therefore, based on the Kuusk (1985) approach, we propose the adaptation of AddingS to the discrete case. The extended model is called AddingSD. This model allows both to conserve the energy and to take into account the hot spot effect between diffuse fluxes. As AddingS/AddingSD are based on adding method then they need a long running time for that in this study, we benefit from both the rapidity of the SAIL++ as well as the hot spot modeling in the AddingSD and we propose a new other approach. This approach is based on the traking of the flux created by the first photons collison by leaves. The analysis of this flux will be done using AddingSD and the RT problem resolution will be based on SAIL++.

The chapter is divided up as follows. First, we present the theoretical background of our models (Section 2). Then, we show model implementation (Section 3), and some validation results (Section 4). Finally, we present our main conclusions and perspectives (Section 5).

2. Theoretical background

In this section, we will first present the models AddingS/AddingSD then we expose our model based on flux decomposition.

2.1 AddingS/AddinSD modeling

The Adding method is based on the assumption that a vegetation layer receiving a radiation flux from bottom or top, partially absorbs it and partially scatters it upward or downward, independently of the other layers (Cooper et al., 1982; Van de Hulst, 1980). Thus, the relationships between fluxes are given by operators which allow the calculation of the output flux density distribution as a function of the input flux density distribution. As the Adding method vegetation layer operators depend on the bidirectional reflectance and transmittance, we propose to derive them both in the turbid and the discrete case based on respectively SAIL and the Kuusk definition of the Hot Spot.

In this section, we first present the Adding operator definition, and secondly the derivation of the bidirectional reflectance and transmittance of a vegetation layer in both turbid and discrete cases corresponding respectively to the operators of the models AddingS and AddingSD.

2.1.1 Adding operators reformulation in the continuous case

In this paragraph, we present a generalization of the Adding operators presented in (Cooper et al., 1982) in the continuous case, dealing with radiance hemispherical distribution.

For a given medium having two parallel sides (top and bottom) receiving a source radiation flux $dE_i(\Omega_i = (\theta_i, \varphi_i))$ (θ_i the zenithal angle and φ_i the azimuthal angle) provided within a cone of solid angle $d\Omega_i = \sin(\theta_i)d\theta_i d\varphi_i$, produces elementary radiances at the top and the bottom of the medium called respectively $dL_e(\Omega_i, \Omega_e)$ and $dL'_e(\Omega_i, \Omega'_e)$ in the directions $\Omega_e = (\theta_e, \varphi_e)$ and $\Omega'_e = (\theta_{e'}, \varphi_{e'})$, respectively.

So the BRDF, r, and the bidirectional transmittance distribution function (BTDF), t, are defined respectively as follows:

$$
\begin{aligned}
r(\Omega_i \rightarrow \Omega_e) &= \frac{\pi dL_e(\Omega_i, \Omega_e)}{dE_i(\Omega_e)} = \frac{\pi dL_e(\Omega_i, \Omega_e)}{L_i(\Omega_i)\cos(\theta_i)d\Omega_i}, \\
t(\Omega_i \rightarrow \Omega_{e'}) &= \frac{\pi dL'_e(\Omega_i, \Omega_{e'})}{dE_i(\Omega_i)} = \frac{\pi dL'_e(\Omega_i, \Omega'_e)}{L_i(\Omega_i)\cos(\theta_i)d\Omega_i}.
\end{aligned}
\tag{1}
$$

where L_i is the radiance provided by the source.

So, we define the two scattering operators $\mathcal{R}$ and $\mathcal{T}$, that give the outward radiance L_e from an incident radiance defined over the whole hemisphere L_i:

$$
\mathcal{R}[L_i](.) = \frac{1}{\pi} \overbrace{\int_{\Pi}}^{\text{Over hemisphere}} r(\Omega_i \rightarrow .)L_i(\Omega_i)\cos(\theta_i)d\Omega_i,
\tag{2}
$$

$$
\mathcal{T}[L_i](.) = \frac{1}{\pi} \int_{\Pi} t(\Omega_i \rightarrow .)L_i(\Omega_i)\cos(\theta_i)d\Omega_i.
\tag{3}
$$

For two medium 1 and 2 such that the second one is above the first one, the top reflectance operator for the canopy is given by (Verhoef, 1985):

$$
\mathcal{R}_t = \mathcal{R}_{t,2} + \mathcal{T}_{u,2} \circ (I - \mathcal{R}_{t,1} \circ \mathcal{R}_{b,2})^{-1} \circ \mathcal{R}_{t,1} \circ \mathcal{T}_{d,2}.
\tag{4}
$$

where $\mathcal{T}_{u,2}$, $\mathcal{T}_{d,2}$ are respectively the upward and downward transmittances of the layer 2, $\mathcal{R}_{t,1}$ and $\mathcal{R}_{b,1}$ are the reflectances of respectively the top of layer 1 and the bottom of layer 2, and I is the identity operator.

Finally, to be implemented such operators have to discretized. Thus, Kallel et al. (2008) propose a regular discretization of the zenithal angle θ and azimuthal angle φ into 20 and 10 intervals respectively. In this case, the reflectance and transmittance operators become matrices and the '$\circ$' operator becomes matrix multiplication.

2.1.2 Turbid case: AddingS

For one vegetation layer, the top and bottom reflectance operators and the downward and upward transmittance operators require the estimation of top and bottom bidirectional reflectances, the downward and upward bidirectional transmittance respectively, r_t, r_b, t_d and t_u. Now, assuming that the vegetation layer is formed by small and flat leaves with uniform azimuthal distribution, the layer has the same response when observed from the top or the bottom. $r_b = r_t$ and $t_u = t_d$. Moreover, two kinds of transmittances can be distinguished: those provided from the extinction of the incident flux, and those provided by the scattering of the incident flux by the vegetation components. So, we called them respectively $t_{.,s}$ and $t_{.,d}$, where . equals d (downward) or u (upward).

The SAIL model allows the BRDF (r_t) and the BTDF by scattering ($t_{d,d}$) derivation of a vegetation layer. Moreover, Kallel et al. (2008) showed that

$$
t_{d,s}(\Omega_i \rightarrow \Omega_{e'}) = \frac{\tau_{ss}\delta(\theta'_e = \theta_i)\delta(\varphi'_e = \varphi_i)}{\cos(\theta_i)\sin(\theta_i)},
\tag{5}
$$

with τ_{ss} the direct transmittance given by SAIL.

As such a model is based on SAIL which assumes that the diffuse fluxes are semi-isotropic, then it is only correct for thin layers ($\mathrm{LAI} < 10^{-2}$) where the diffuse fluxes contribution to the BRDF/BTDF are small. Therefore, to estimate the reflectance of a thick layer and overcome the semi-isotropy assumption, we propose to divide the thick layer into thin sublayers with LAI value, $\mathrm{L_{min}} = 10^{-3}$. The whole layer reflectance operator is then derived with good accuracy using the adding method Eq. (4) as it allows to model the diffuse flux anisotropy.

2.1.3 Discrete case: AddingSD

In the discrete case, the size of the leaves is no longer assumed null and there is a non-negligible correlation between the incident flux path and the diffused flux: the hot spot effect Kuusk (1985); Suits (1972). Until now, such an effect was taken into account in 1-D model only for the single scattering contribution from soil and foliage that is increased. Now, as the diffuse fluxes are not decreased consequently, the radiative budget is not checked. Now, the hot spot effect occurs also for diffuse fluxes (whose contribution increases with the vegetation depth). We call such a phenomena the multi hot spot effect. In this section, having recall Kuusk' model Kuusk (1985), we present our approach.

2.1.3.1 Kuusk' model

For a layer located at in altitude between -1 and 0, the single scattering reflectance ($\rho_{HS}^{(1)}$) by a leaf M at depth z, for the source and observation directions being respectively Ω_s and Ω_o, is (Verhoef (1998), pp 150-159):

$$\rho_{HS}^{(1)}(z) = P_{so}(\Omega_s, \Omega_o, z) \frac{w(\Omega_s, \Omega_o)}{\pi}, \qquad (6)$$

where w is the bidirectional scattering parameter under the vegetation (Verhoef, 1984) and $P_{so}(\Omega_s, \Omega_o, z)$ is the conjoint probability that the incident flux reaches M without any collision with other canopy components and that, after scattering by M, it also reaches the top of the canopy without collisions Kuusk (1985):

$$
\begin{aligned}
P_o(\Omega_s, \Omega_o, z) &= \exp\left[-\int_z^0 \{k + K - \sqrt{Kk}\exp[(z-x)b]\}\mathrm{d}x \right], \\
&= \exp[(K+k)z]C_{HS}(\Omega_s, \Omega_o, z),
\end{aligned}
\qquad (7)
$$

with k, K the extinction respectively in source and observation directions and C_{HS} the correction factor:

$$C_{HS}(\Omega_s, \Omega_o, z) = \exp\left[\frac{\sqrt{kK}}{b}[1 - \exp(bz)] \right], \qquad (8)$$

where b is a function of the vegetation features, the different solid angles and the hot spot factor d_l defined as the ratio between the leaf radius and the layer height Kuusk (1985); Pinty et al. (2004).

2.1.3.2 Multi hot spot model

Firstly recall that the energy conservation is insured by adding model whatever be the foliage area volume density (FAVD), u_l (cf. Appendix B) or the probability of finding foliage P_χ. In this subsection, we first show that the first order hot spot corresponds to the use of a fictive equivalent P_χ, called $P_{\chi,HS}$.

For a vegetation layer composed of two layers: a thin layer 2 above a layer 1, located respectively in $[z_0, 0]$ and $[-1, z_0]$, let $P_{so}(\Omega_s, \Omega_o, z_0, z)$ denotes the joint probability that the two fluxes do not collide with leaves for $z' \in [z_0, 0]$ (only in the layer 2). Its expression is obtained from Eq. (7) by changing the integral endpoints $[z, 0]$ by $[z_0, 0]$:

$$P_{so}(\Omega_s, \Omega_o, z_0, z) = \exp[(K+k)z_0]\mathcal{C}_{HS}(\Omega_s, \Omega_o, z_0, z),$$

with $\mathcal{C}_{HS}$ the generalized correction factor:

$$\mathcal{C}_{HS}(\Omega_s, \Omega_o, z_0, z) = \exp\left[\frac{\sqrt{kK}}{b}\left(\exp[b(z-z_0)] - \exp[bz]\right)\right].$$

The conditional probability definition that the flux in the direction Ω_o does not collide leaves given the same property for the incident flux is:

$$P_o(\Omega_o|\Omega_s, z_0, z) = \frac{P_{so}(\Omega_s, \Omega_o, z_0, z)}{P_s(\Omega_s, z_0)},$$

where $P_s(\Omega_s, z_0)$ represents the prior probability of gap in the direction Ω_s. Since $P_s(\Omega_s, z_0) = \exp[kz_0]$, then:

$$P_o(\Omega_o|\Omega_s, z_0, z) = \exp[Kz_0]\mathcal{C}_{HS}(\Omega_s, \Omega_o, z_0, z).$$

In the case of the direct flux, the first order contribution of a leaf $M(z)$ in the layer 1 to the BRDF is:

$$\rho_{HS}^{(1)}(z) = \underbrace{\exp[kz_0]}_{P_s(\Omega_s, z_0)}\underbrace{\rho_{HS}^{(1)}(z-z_0)}_{\text{layer 1}}\underbrace{\exp\{\overbrace{Kz_0 + \log[\mathcal{C}_{HS}(\Omega_s, \Omega_o, z_0, z)]}^{K_{HS}(\Omega_o|\Omega_s, z_0, z)z_0}\}}_{P_o(\Omega_o|\Omega_s, z_0, z)}. \tag{9}$$

In Eq. (9), $\rho_{HS}^{(1)}(z)$ can be interpreted as follows: reaching the top of the canopy the direct flux is partially extinguished in the layer 2 by the factor $P_s(\Omega_s, z_0)$. Then, reaching the interface between the two layers, its amplitude will be determined according to $\rho_{HS}^{(1)}(z-z_0)$ that depends on the layer 1 features. Finally, $K_{HS}(\Omega_o|\Omega_s, z_0, z)$ can be viewed as the 'effective' extinction related to the conditional probability of gap $P_o(\Omega_o|\Omega_s, z_0, z)$ of the layer 2. Indeed, $K_{HS} < K$ means that the probability of collision with leaves (or probability of finding leaves, P_χ) for the exiting flux that it will be noted $L_{o,HS}^{(1)}$, is decreased. Since the extinction depends linearly on P_χ, one can deem that P_χ is locally decreased by the factor $\gamma = \frac{K_{HS}}{K}$:

$$P_{\chi,HS}(\Omega_o|\Omega_s, z_0, z) = \frac{K_{HS}(\Omega_o|\Omega_s, z_0, z)}{K}P_\chi. \tag{10}$$

The physical interpretation of $P_{\chi,HS}$ is as follows. Assume that the probability of gap (for a given flux) is increased in the layer 2. For this flux, the 'effective' probability of being collided by vegetation when crossing the layer is reduced accordingly. Obviously, the fist collision between the flux and the vegetation is reduced according to the same probabilty of finding vegetation or similarly the same density of vegetation. Now, since the layer 2 is thin, its corresponding reflectance and diffuse transmittance depend mainly on the first interaction. So, just an approximation of the multiple scattered fluxes is sufficient to derive the layer 2 scattering terms with good accuracy. For that, the derivation of all diffuse fluxes can be done using this 'effective' probability of finding foliage ($P_{\chi,HS}$ in our case). Moreover, for such a modeling, the

interactions of the considered flux and the layer 2 components (transmittance by extinction, reflectance and diffuse transmittance) are derived using exactly the same probability value ($P_{\chi,HS}$), which is physically consistent and thus leads to the conservation of the energy of this flux. Furthermore, by doing the same processing for all fluxes exiting the layer 1 in direction of the layer 2, the energy of all fluxes is conserved and so the energy is conserved in the system composed by the two vegetation layers.

The layer 2 reflectance and diffuse transmittance of the flux $L_{o,HS}^{(1)}$, respectively called $r_{b,2,HS}(z, \Omega_o \rightarrow .)$ and $t_{d,2,HS}(z, \Omega_o \rightarrow .)$, have therefore to be estimated using $P_{\chi,HS}$ rather than the initial P_χ. The first order hot spot effect can then be viewed as a local reduction of the layer 2 probability of finding leaves. The layer 2 operators are derived accordingly, and the two layer reflectance operator is obtained using Eq. (4). In summary, given a vegetation layer, its corresponding reflectance is computed dividing it into N_{HS} thin sublayers with a value of LAI, $L_{HS} = 3 \times 10^{-2}$ (L_{HS} is higher than the elementary sublayer LAI corresponding to AddingS model concatenation, $L_{min} = 10^{-3}$) and iteratively adding a new sublayer to the current 'stack' of sublayers (from 1 to N_{HS}).

More precisely, beginning from a thin layer, where the neglecting of the hot spot effect appears reasonable, thin layers are added, one after one, to build up a 'system' taking into account the whole hot spot effect (as well as conserving the energy). The contribution of each new sublayer 2 to the high order hot spot effect is computed as follows. The flux reaching the top of the layer 2 is scattered many times before reaching the interface between the two layers where it is considered again as a direct flux (according to the adding method). In layer 1, the first order (direct flux case) hot spot computation is therefore valid. Adding iteratively the thin layers and the contribution of their diffuse fluxes, the hot spot effect between all the diffuse fluxes is taken into account.

Finally, for more information about the implementation of the models AddingS/AddingSD, readers are invited to read the article (Kallel et al., 2008).

2.2 Virtual flux decomposition

In this section, we propose an alternative to AddingSD that is simpler, conserves the energy and based on effective vegetation density too but does not take into account the high order hot spot effect. Moreover, the proposed approach is an extension to the discrete case of SAIL++, that we provide an overview in Appendix A. To do the extension, we study the collision of direct fluxes with vegetation in the discrete homogeneous medium case. The energy will be conserved by increasing the flux created by first collision and decreasing the flux created by this flux scattering.

2.2.1 Derivation of $L_+^{1,n}$

Figure 1 shows two points $M(x, y, z)$ and $N(x', y', t)$ in a vegetation layer assumed be a homogeneous discrete medium such that $t < z$. The elementary volume at M is viewed from N at an elementary solid angle $d\Omega$ with $\Omega = (\theta, \varphi)$. A direct flux ($E_s(0)$) present above the vegetation layer having direction $\Omega_s = (\theta_s, 0)$ passes through the vegetation from the top to N without a collision. By assuming a constant extinction k along the path, E_s at altitude t is

$$E_s(t) = E_s(0) \exp(kt). \tag{11}$$

Then the light is scattered in an elementary volume at N with an elementary thickness dt. Thus scattered radiance in the direction $d\Omega$ called ($dL_+^1(N, \Omega)$) is

$$dL_+^1(N, \Omega) = E_s(t)\pi^{-1}w(\Omega_s \rightarrow \Omega)dt. \tag{12}$$
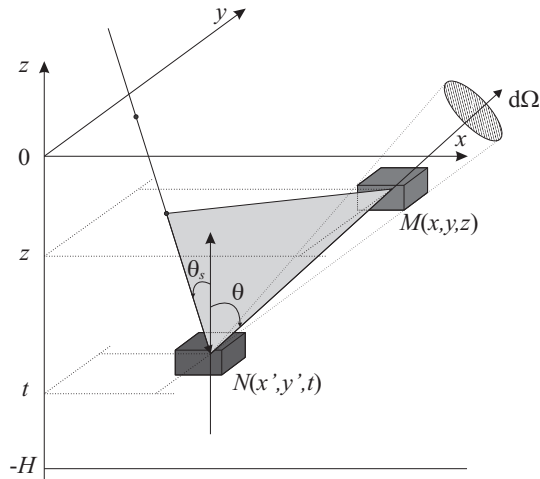
Fig. 1. A vegetation layer located from altitude 0 to $-H$ and assumed a discrete medium. Two point $M(x,y,z)$ and $N(x',y',z)$ are located in the layer. The elementary volume at M is viewed from N under an elementary solid angle $(d\Omega)$ with a polar angle θ. A direct flux with zenith angle θ_s collides with vegetation in an elementary volume at point N, is then reflected in the solid angle $d\Omega$ and reaches point M without collision. The downward and upward paths are correlated from altitude z to t as shown by the gray triangle linking the two paths.

$dL^1_+(N,\Omega)$ travels from N to M without collision. Therefore, by assuming a constant extinction κ along the path and without taking into account the dependency between paths, the radiance reaching M called $dL^{1*}_+(N \to M,\Omega)$ is

$$\begin{aligned}
dL^{1*}_+(N \to M,\Omega) &= dL^1_+(N,\Omega)\exp[\kappa(t-z)], \\
&= E_s(0)\exp[(k+\kappa)(t-z)]\exp(kz)\pi^{-1}w(\Omega_s \to \Omega)dt.
\end{aligned} \tag{13}$$

Since the medium is assumed discrete, the hot spot effect representing the dependency between downward direct fluxes and diffuse fluxes at N has to be taken into account from depth t to z. Using Kuusk's model [1985], the radiance reaching M called $dL^1_+(N \to M,\Omega)$ is

$$\begin{aligned}
dL^1_+(N \to M,\Omega) &= dL^{1*}_+(N \to M,\Omega)\exp\left[\frac{\sqrt{k\kappa}}{b}\left(1-\exp[-b(z-t)]\right)\right], \\
&= E_s(0)\exp[(k+\kappa)(t-z)]\exp\left[\frac{\sqrt{k\kappa}}{b}\left(1-\exp[-b(z-t)]\right)\right] \\
&\quad \times \exp(kz)\pi^{-1}w(\Omega_s \to \Omega)dt.
\end{aligned} \tag{14}$$

Eq. (14) is the foundation of our model. However, since it has a complex expression, in particular in the exponential term corresponding to the hot spot correction, there is no linearity versus z and t enabling a simple solution based on differentiel equations as those of SAIL++ [cf. Eqs. 85]. For that, we propose to apply the Taylor series decomposition to this term

$$\exp\left[\frac{\sqrt{k\kappa}}{b}\left(1-\exp[-b(z-t)]\right)\right] = \exp\left[\frac{\sqrt{k\kappa}}{b}\right]\sum_{n=0}^{\infty}\frac{(-1)^n(k\kappa)^{n/2}}{n!b^n}\exp[nb(t-z)]. \tag{15}$$

Therefore, Eq. (14) can be written as follows,

$$dL_+^1(N \to M, \Omega) = \sum_{n=0}^{\infty} (-1)^n A_n dL_+^{1,n}(N \to M, \Omega), \tag{16}$$

where

$$
\begin{aligned}
dL_+^{1,n}(N \to M, \Omega) &= E_s(0) \exp[(k + \kappa_n)(t - z)] \times \exp(kz)\pi^{-1}w(\Omega_s \to \Omega)dt, \\
A_n &= \frac{(k\kappa)^{n/2}}{n!b^n} \exp\left[\frac{\sqrt{k\kappa}}{b}\right], \\
\kappa_n &= \kappa + nb.
\end{aligned}
\tag{17}
$$

As the vegetation is homogeneous, then $dL_+^1(N \to M, \Omega)$ can be written simply as $dL_+^1(t \to z, \Omega)$. Thus, $L_+^1(z, \Omega)$ is obtained by integration of dL_+^1 over the depth $[-H, z]$

$$L_+^1(z, \Omega) = \int_{t=-H}^{z} dL_+^1(t \to z, \Omega). \tag{18}$$

Based on (16), L_+^1 can be written as

$$L_+^1(z, \Omega) = \sum_{n=0}^{+\infty} (-1)^n A_n L_+^{1,n}(z, \Omega), \tag{19}$$

where

$$
\begin{aligned}
L_+^{1,n}(z, \Omega) &= \int_{-H}^{z} E_s(0) \exp[(k + \kappa + nb)(t - z)] \exp(kz)\pi^{-1}w(\Omega_s \to \Omega)dt, \\
&= E_s(0) \frac{1 - \exp[-(k + \kappa + nb)(H + z)]}{k + \kappa + nb} \exp(kz)\pi^{-1}w(\Omega_s \to \Omega).
\end{aligned}
\tag{20}
$$

2.2.2 Application of the effective vegetation density approach

Here, we will try to extend the reformulated SAIL++ equation (cf. Appendix A.3) to the discrete case. Thus, as shown in Section 2.1.3, the hot spot effect will be treated as an increased posterior probability of gap which, in turn, results from a reduction in vegetation density. Then, it was suggested the use of the concept 'effective vegetation density' to describe the phenomenon. In this subsection, we propose to derive this density for $L_+^{1,n}$, $\forall n \in \mathbb{N}$, and to use it further to derive the equations of fluxes created by $L_+^{1,n}$ scattering. Moreover, the same effective density using leads to conserve energy (as explained in Section 2.1.3).

In Eqs. (13) (17), the difference between dL_+^{1*} and $dL_+^{1,n}$ is the value of the extinction in the direction Ω (κ and κ_n respectively). Note that $\forall n > 0$, $\kappa_n > \kappa$, then $dL_+^{1,n}$ decreases faster than dL_+^1.

According to our approach described in Section A, the variation in the extinction factor is linked to the variation of the collision probability locally around M. In other words, a decrease in the probability of finding foliage at M decreases P_χ, accordingly (cf. Appendix B). Now, according to (77) and (99)

$$
\left.
\begin{aligned}
\kappa &= d_L P_\chi(M)\kappa_o \\
\kappa_n &= d_L P_{\chi,n}(M)\kappa_o
\end{aligned}
\right\} \Rightarrow P_{\chi,n}(M) = \frac{\kappa_n}{\kappa} P_\chi(M),
\tag{21}
$$

with $P_{\chi,n}(M)$ the a posteriori probability of finding vegetation at M for the virtual radiance $dL_+^{1,n}$, and κ_0 the normalized extinction factor [as explained in Eq. (77), it is independent on vegetation density]. We will use this notation in the following for SAIL++ scattering parameters. For each scattering parameter X, one can define the corresponding normalized one X_0 according to Eq. (77).

As we can see in Eqs. (21), $P_{\chi,n}(M)$ does not depend on M. Thus, it will be simply called $P_{\chi,n}$. Then, based on L_+^1 differential equation derivation [cf. Eq. (89)] and replacing κ by κ_n, we obtain,

$$
\begin{aligned}
\frac{dL_+^{1,n}(z,\Omega)}{dz} &= [\mathfrak{s} \circ E_s(z,\Omega_s)](\Omega) - \kappa_n L_+^{1,n}(z,\Omega) = [\mathfrak{s} \circ E_s(z,\Omega_s)](\Omega) - d_L P_{\chi,n}\kappa_0 L_+^{1,n}(z,\Omega), \\
&= [\mathfrak{s} \circ E_s(z,\Omega_s)](\Omega) - d_L P_{\chi,n}[\mathfrak{k}_0 \circ L_+^{1,n}(z)](\Omega),
\end{aligned}
\tag{22}
$$

where $\mathfrak{k}_0$ is the normalized scattering term corresponding to $\mathfrak{k}$ [cf. Eq. (80)].

It leads to the following important result linking the differentiation of L_+^1 to $(L_+^{1,n})_{n\in\mathbb{N}}$:

$$
\begin{aligned}
\frac{dL_+^1(z,\Omega)}{dz} &= \frac{d\left\{\sum_{n=0}^{+\infty}(-1)^n A_n L_+^{1,n}(z,\Omega)\right\}}{dz}, \\
&= \sum_{n=0}^{+\infty}(-1)^n A_n\left\{[\mathfrak{s}\circ E_s(z,\Omega_s)](\Omega) - d_L P_{\chi,n}[\mathfrak{k}_0 \circ L_+^{1,n}(z)](\Omega)\right\}, \\
&= [\mathfrak{s}\circ E_s(z,\Omega_s)](\Omega)\overbrace{\sum_{n=0}^{+\infty}(-1)^n A_n}^{=1} - d_L\sum_{n=0}^{+\infty}(-1)^n A_n P_{\chi,n}[\mathfrak{k}_0 \circ L_+^{1,n}(z)](\Omega), \\
&= [\mathfrak{s}\circ E_s(z,\Omega_s)](\Omega) - d_L\sum_{n=0}^{+\infty}(-1)^n A_n P_{\chi,n}[\mathfrak{k}_0 \circ L_+^{1,n}(z)](\Omega).
\end{aligned}
\tag{23}
$$

Thus, the radiance distributions created by $dL_+^{1,n}$ scattering depend on $P_{\chi,n}$ rather than P_χ. As explained in Appendix A.3, these radiances are the downward diffuse radiance distribution (L_-), upward higher order diffuse radiance distribution (L_+^∞), upward radiance in observation direction (E_o^+) and downward radiance in observation direction (E_o^-). Note that, the mathematical validation, in term of global flux estimation, is explained in Subsection 2.2.3 and then shown in Appendix C.

Note that, similar to L_+^1, the differentiation of E_o^+ that depends only on E_s is

$$
\frac{dE_o^+(z,\Omega_o)}{dz} = w E_s(z,\Omega_s) - d_L\sum_{n=0}^{+\infty}(-1)^n A_n P_{\chi,n} K_0 E_0^{+,n}(z,\Omega_o),
\tag{24}
$$

with Ω_o the E_s direction, K the extinction factor in the direction Ω_o and

$$
E_o^{+,n}(z,\Omega_o) = E_s(0)\frac{1 - \exp[-(k+K+nb)(H+z)]}{k+K+nb}\exp(kz)w(\Omega_s \to \Omega_o).
\tag{25}
$$

As in classical models, there is no need to use Eq. (24). We merely assume, as in the turbid case, that

$$
\frac{dE_0^+(z,\Omega_o)}{dz} = w E_s(z,\Omega_s) - K E_0^+(z,\Omega_o),
\tag{26}
$$

and the reflectance provided from the first order collision ($\rho_{so}^{(0),HS}$) will be corrected using the tradional formula (Kuusk, 1985)

$$\rho_{so}^{(0),HS} = w \int_{-H}^{0} \exp\left[(k+K)z + \frac{\sqrt{kK}}{b}[1 - \exp(bz)]\right] dz. \tag{27}$$

2.2.3 Dependency on $L_+^{1,n}$

In this subsection, we propose a modification to the reformulated SAIL++ equation set, presented in Appendix A.3, in order to take into account the effective vegetation density values in the expressions of L_-, L_+^∞, E_o^+ and E_o^- that depend on $L_+^{1,n}$ scattering.

First, let us derive the angular differentiation of E_o^+ ($d^2 E_o^+(z, \Omega \to \Omega_o)$) that depends only on $L_+^{1,n}$. Compared to the dependency on L_+ in classical SAIL++ equations, P_χ has to be replaced by $P_{\chi,n}$. Thus,

$$\frac{d[d^2 E_o^+(z, \Omega \to \Omega_o)]}{dz} = w_n'(\Omega \to \Omega_o)L_+^{1,n}(z,\Omega)\cos(\theta)d\Omega, \tag{28}$$

where

$$w_n'(\Omega \to \Omega_o) = d_L P_{\chi,n} w_0'(\Omega \to \Omega_o), \tag{29}$$

with w_0' the normalized scattering parameter corresponding to w' [cf. Eq. (76)].

Then, the angular differentiation of E_o^+ ($d^2 E_o^+(z, \Omega \to \Omega_o)$) which depends only on L_+^1 is obtained by summing the contribution of the set $(L_+^{1,n})_{n\in\mathbb{N}}$

$$\frac{d[d^2 E_o^+(z, \Omega \to \Omega_o)]}{dz} = \sum_{n=0}^{+\infty} (-1)^n A_n w_n'(\Omega \to \Omega_o)L_+^{1,n}(z,\Omega)\cos(\theta)d\Omega. \tag{30}$$

Note that, based on AddingSD formalism, the validity of our decomposition in this derivation of $P_{\chi,n}$ is shown in Appendix C.

By integration of Ω over the upper-hemisphere [cf. Eqs. (75) (84)], Eq. (30) becomes

$$\begin{aligned}
\frac{dE_o^+(z, \Omega_o)}{dz} &= d_L \sum_{n=0}^{+\infty} (-1)^n A_n P_{\chi,n} \int_\Pi w_0'(\Omega \to \Omega_o)L_+^{1,n}(z,\Omega)\cos(\theta)d\Omega, \\
&= d_L \sum_{n=0}^{+\infty} (-1)^n A_n P_{\chi,n}[\mathfrak{v}_0' \circ L_+^{1,n}(z)],
\end{aligned} \tag{31}$$

with $\mathfrak{v}_0'$ the normalized scattering parameter corresponding to $\mathfrak{v}'$ [cf. Eq. (74)].

Next, by integrating the dependency on E_s, L_- and L_+^∞, the original reformulated SAIL++ Eq. (92) becomes

$$\frac{dE_o^+}{dz} = wE_s + \mathfrak{v} \circ L_- + \mathfrak{v}' \circ L_+^\infty + d_L \sum_{n=0}^{+\infty} (-1)^n A_n P_{\chi,n}[\mathfrak{v}_0' \circ L_+^{1,n}(z)] - KE_o^+. \tag{32}$$

Similarly, Eqs. (91), (90) and (93) become respectively

$$\begin{aligned}
\frac{dL_-}{dz} &= -\mathfrak{s}' \circ E_s + \mathfrak{A} \circ L_- - \mathfrak{B} \circ L_+^\infty - d_L \sum_{n=0}^{+\infty} (-1)^n A_n P_{\chi,n}[\mathfrak{B}_0 \circ L_+^{1,n}(z)], \\
\frac{dL_+^\infty}{dz} &= \mathfrak{o} \circ E_s + \mathfrak{B} \circ L_- - \mathfrak{A} \circ L_+^\infty + d_L \sum_{n=0}^{+\infty} (-1)^n A_n P_{\chi,n}[\mathfrak{B}_0' \circ L_+^{1,n}(z)], \\
\frac{dE_o^-}{dz} &= -w' E_s - \mathfrak{v}' \circ L_- - \mathfrak{v} \circ L_+^\infty - d_L \sum_{n=0}^{+\infty} (-1)^n A_n P_{\chi,n}[\mathfrak{v}_0 \circ L_+^{1,n}(z)] + KE_o^-,
\end{aligned} \tag{33}$$

with o the vacuum operator, $\mathfrak{B}_0$, $\mathfrak{B}_0'$ and $\mathfrak{v}_0$ the normalized scattering parameters corresponding to $\mathfrak{B}$, $\mathfrak{B}'$ and $\mathfrak{v}$ [cf. Eqs. (73) (74) (75)], respectively.

3. Virtual flux decomposition implementation

As in SAIL++ (cf. Appendix A.2), the implementation needs the discretization of the diffuses fluxes over the hemispheres. These diffuse fluxes correspond to the diffuse radiances $(L_+^{1,n})_{n\in\mathbb{N}}$, L_+^{∞} and L_- when only a vegetation layer is considered (cf. Subsection 2.2). The corresponding discrete fluxes will be called $(E_+^{1,n})_{n\in\mathbb{N}}$, E_+^{∞} and E_-, respectively. The reflectances created by scattering of $(E_+^{1,n})_{n\in\mathbb{N}}$ and $(E_+^{0,n})_{n\in\mathbb{N}}$ will be separated to the one created by E_s. The separation enables the solution of the RT problem based on SAIL++ formalism.

First, we present the processing of the vegetation layer. Second, we show the soil vegetation coupling.

3.1 Vegetation layer
3.1.1 $E_+^{1,n}$ estimation

As reformulated in Appendix A.3, the difference between SAIL ++ and our model occurs in the calculation of L_+^1. In our model it is decomposed into the sequence $(L_+^{1,n})_{n\in\mathbb{N}}$ thus modifying the expressions of L_-, L_+^{∞}, E_o^+ and E_o^-. Therefore, in this section, we propose the derivation of a new expression for the discrete fluxes E_- and E_+^{∞} as well as the radiances E_o^+ and E_o^- versus $(E_+^{1,n})_{n\in\mathbb{N}}$.

Now, $\forall n \in \mathbb{N}, L_+^{1,n}$ is given by Eq. (20). Let us consider the Verhoef (1998) sphere tessellation into N segments, then the irradiance $E_{+,i}^{1,n}$ of each segment i is

$$
\begin{aligned}
E_{+,i}^{1,n}(z) &= \int_{\Delta\Omega_i} L_+^{1,n}(z,\Omega)\cos(\theta)\mathrm{d}\Omega, \\
&\approx E_s(0)\frac{1-\exp[-(k+\langle\kappa\rangle_{\Delta\Omega_i}+n\langle b\rangle_{\Delta\Omega_i})(H+z)]}{k+\langle\kappa\rangle_{\Delta\Omega_i}+n\langle b\rangle_{\Delta\Omega_i}}\exp(kz) \\
&\quad\times \int_{\Delta\Omega_i}\pi^{-1}w(\Omega_s\rightarrow\Omega)\cos(\theta)\mathrm{d}\Omega,
\end{aligned}
\tag{34}
$$

where $\langle.\rangle_{\Delta\Omega_i}$ is the mean value operator defined for a given function f as follows

$$
\langle f(\Omega)\rangle_{\Delta\Omega_i} = \frac{\int_{\Omega\in\Delta\Omega_i}f(\Omega)\cos(\Omega)\mathrm{d}\Omega}{\int_{\Omega\in\Delta\Omega_i}\cos(\Omega)\mathrm{d}\Omega}.
\tag{35}
$$

Following Verhoef (1998) terminology,

$$
\begin{aligned}
\langle\kappa\rangle_{\Delta\Omega_i} &= \boldsymbol{\kappa}(i), \\
\int_{\Delta\Omega_i}\pi^{-1}w(\Omega_s\rightarrow\Omega)\cos(\theta)\mathrm{d}\Omega &= \mathbf{s}(i),
\end{aligned}
\tag{36}
$$

similarly, we adopt the following notation

$$
\langle b\rangle_{\Delta\Omega_i} = \boldsymbol{b}(i),
\tag{37}
$$

thus κ_n [cf. Eq. (17)] will be extended in the discrete case as follows

$$
\boldsymbol{\kappa}_n(i) = \boldsymbol{\kappa}(i) + n\boldsymbol{b}(i).
\tag{38}
$$

3.1.2 $E_{+,i}^{1,n}$ dependency

Being scattered, $E_{+,i}^{1,n}$ can create both diffuse fluxes E_+^∞ and E_- as well as radiances E_o^+ and E_o^-. The scattering parameters will be called respectively $\mathbf{s}_{i,n}$, $\mathbf{s}'_{i,n}$, $w'_{i,n}$ and $w_{i,n}$. Now,

$$w'_{i,n}(\Omega_o) = d_L P_{\chi,n} \langle w'_0(\Omega \to \Omega_o) \rangle_{\Omega \in \Delta\Omega_i} = P_{\chi,n} \mathbf{v}'_0(i), \tag{39}$$

where $\mathbf{v}'_0$ is the normalized SAIL++ scattering parameter corresponding to $\mathbf{v}'$ [cf. Eq. (85)]. Similarly, one can define $w_{i,n}$ the analogue of $w'_{i,n}$ when $\Delta\Omega_i$ and Ω_o are in the same hemisphere

$$w_{i,n}(\Omega_o) = d_L P_{\chi,n} \langle w_0(\Omega \to \Omega_o) \rangle_{\Omega \in \Delta\Omega_i} = P_{\chi,n} \mathbf{v}_0(i), \tag{40}$$

where $\mathbf{v}_0$ is the normalized scattering parameter corresponding to $\mathbf{v}$ [cf. Eq. (85)].
As in the SAIL++ model (Verhoef, 1998), $\mathbf{s}_{i,n}$ and $\mathbf{s}'_{i,n}$ are integrated values of $w_{i,n}$ and $w'_{i,n}$ over the output solid angle. So, for $m \in \{1, \ldots, N\}$ a given discrete solid angle index

$$\begin{aligned}
\mathbf{s}_{i,n}(m) &= \int_{\Delta\Omega_m} w_{i,n}(\Omega_m) \mathrm{d}\Omega_m = d_L P_{\chi,n} \pi^{-1} \langle\langle w_0(\Omega \to \Omega_+) \rangle\rangle_{(\Omega,\Omega_+) \in (\Delta\Omega_i, \Delta\Omega_m)} \frac{2\pi}{N}, \\
&= d_L P_{\chi,n} \mathbf{B}'_0(i \to m),
\end{aligned} \tag{41}$$

where $\mathbf{B}'_0$ is the normalized SAIL++ scattering matrix corresponding to $\mathbf{B}'$ [cf. Eq. (86)]. Similarly,

$$\mathbf{s}_{i,n}(m) = d_L P_{\chi,n} \mathbf{B}_0(i \to m), \tag{42}$$

where $\mathbf{B}_0$ is the normalized scattering matrix corresponding to $\mathbf{B}$ [cf. Eq. (85)].

3.1.3 $E_{+,i}^{1,n}$ decomposition

From Eq. (34), one has

$$\begin{aligned}
E_{+,i}^{1,n}(z) &= E_s(0) \frac{1 - \exp[-(k + \boldsymbol{\kappa}_n(i))(H + z)]}{k + \boldsymbol{\kappa}_n(i)} \exp(kz) \mathbf{s}(i), \\
&= X_i^n E_{+,i,1}^{1,n}(z) + Y_i^n E_{+,i,2}^{1,n}(z).
\end{aligned} \tag{43}$$

with

$$\begin{aligned}
X_i^n &= \frac{\mathbf{s}(i)}{k + \boldsymbol{\kappa}_n(i)}, \\
Y_i^n &= -\frac{\mathbf{s}(i) \exp(-kH)}{k + \boldsymbol{\kappa}_n(i)}, \\
E_{+,i,1}^{1,n}(z) &= E_s(0) \exp(kz) = E_s(z), \\
E_{+,i,2}^{1,n}(z) &= E_s(0) \exp[-\boldsymbol{\kappa}_n(i)(H + z)].
\end{aligned} \tag{44}$$

Therefore, $E_{+,i,1}^{1,n}$ and $E_{+,i,2}^{1,n}$ can be viewed as the direct downward and upward fluxes with an extinction factor under the vegetation equal to k and $\boldsymbol{\kappa}_n(i)$, respectively.

Thus, the corresponding RT discrete equation set to the continuous Eqs. (32) (33) presented in the last section is

$$
\begin{cases}
E_{+,i,1}^{1,n}(0) = E_{+,i,2}^{1,n}(-H) = E_s(0), \forall\{i,n\} \in \{1,\dots,N\} \times \mathbb{N}, \\
\dfrac{dE_s}{dz} = kE_s, \\
\dfrac{dE_{+,i,1}^{1,n}}{dz} = kE_{+,i,1}^{1,n}, \forall\{i,n\} \in \{1,\dots,N\} \times \mathbb{N}, \\
\dfrac{dE_{+,i,2}^{1,n}}{dz} = -\boldsymbol{\kappa}_n(i)E_{+,i,2}^{1,n}, \forall\{i,n\} \in \{1,\dots,N\} \times \mathbb{N}, \\
\dfrac{dE_-}{dz} = -\mathbf{s}'E_s + \mathbf{A}E_- - \mathbf{B}E_+ - \displaystyle\sum_{n=0}^{\infty}(-1)^n \sum_{i=1}^{N} A_i^n(X_i^n \mathbf{s}_{i,n}E_{+,i,1}^{1,n} + Y_i^n \mathbf{s}_{i,n}E_{+,i,2}^{1,n}), \\
\dfrac{dE_+^{\infty}}{dz} = \mathbf{B}E_- - \mathbf{A}E_+ + \displaystyle\sum_{n=0}^{\infty}(-1)^n \sum_{i=1}^{N} A_i^n(X_i^n \mathbf{s}_{i,n}'E_{+,i,1}^{1,n} + Y_i^n \mathbf{s}_{i,n}'E_{+,i,2}^{1,n}), \\
\dfrac{dE_o^+}{dz} = wE_s + \mathbf{v}E_- + \mathbf{v}'E_+ + \displaystyle\sum_{n=0}^{\infty}(-1)^n \sum_{i=1}^{N} A_i^n(X_i^n w_{i,n}'E_{+,i,1}^{1,n} + Y_i^n w_{i,n}'E_{+,i,2}^{1,n}) - KE_o^+, \\
\dfrac{dE_o^-}{dz} = -w'E_s - \mathbf{v}'E_- - \mathbf{v}E_+ - \displaystyle\sum_{n=0}^{\infty}(-1)^n \sum_{i=1}^{N} A_i^n(X_i^n w_{i,n}E_{+,i,1}^{1,n} + Y_i^n w_{i,n}E_{+,i,2}^{1,n}) + KE_o^-,
\end{cases}
\tag{45}
$$

with A_i^n the extension of A_n to the discrete case Eq. (17)

$$
A_i^n = \frac{(k\boldsymbol{\kappa}(i))^{n/2}}{n!\boldsymbol{b}(i)^n} \exp\left[\frac{\sqrt{k\boldsymbol{\kappa}(i)}}{\boldsymbol{b}(i)}\right].
\tag{46}
$$

From a mathematical perspective, System 45 could be viewed as follows. The unknowns are E_-, E_+^{∞}, E_o^+ and E_o^-. They have to be solved using three differential equations linking them (three last Equations in Set 45). In addition to the unknown functions, the differential equations contain additive terms composed of linear combinations of known functions which are E_s and $E_{+,i,j}^{1,n}, \forall\{i,j,n\} \in \{1,\dots,N\} \times \{1,2\} \times \mathbb{N}$. Therefore, solutions to the global differential equation set (E_-, E_+^{∞}, E_o^+ and E_o^-) can be written as linear combinations (the same as the combination of the additive terms in the initial set) of the same differential equation set solutions with only one additive term among the set E_s, $E_{+,i,j}^{1,n}, \forall\{i,j,n\} \in \{1,\dots,N\} \times \{1,2\} \times \mathbb{N}$.

Therefore, we propose the following solution. E_-, E_+^{∞}, E_o^+ and E_o^- have to be derived for different sources: $E_s(0)$, $E_{+,i,1}^{1,n}(0)$ and $E_{+,i,2}^{1,n}(-H)$, $\forall\{i,n\} \in \{1,\dots,N\} \times \mathbb{N}$. For that, one can define the corresponding sub-solutions which are E_-^s, $E_+^{\infty,s}$, $E_o^{+,s}$, $E_o^{-,s}$, $\forall\{i,j,n\} \in \{1,\dots,N\} \times \{1,2\} \times \mathbb{N}$, $E_{-,i,j}^n$, $E_{+,i,j}^{\infty,n}$, $E_{o,i,j}^{+,n}$ and $E_{o,i,j}^{-,n}$, respectively.

According to Eqs. (45), the global solution for $E \in \{E_-, E_+^{\infty}, E_o^+, E_o^-\}$ is written as follows

$$
E = E^s + \sum_{n=0}^{\infty}(-1)^n \sum_{i=1}^{N} A_i^n(X_i^n E_{i,1}^n + Y_i^n E_{i,2}^n),
\tag{47}
$$

Now, compared to SAIL++ in terms of boundary conditions (cf. Appendix A.2), each term x of the boundary condition matrix [cf. Eq. (87)] that depends on the direct source flux [cf. Eq.

(88)], i.e.

$$x \in \left\{ \tau_{ss} = \frac{E_s(-H)}{E_s(0)}, \boldsymbol{\tau}_{sd} = \frac{E_-(-H)}{E_s(0)}, \boldsymbol{\rho}_{sd} = \frac{E_+^0(0) + E_+^\infty(0)}{E_s(0)}, \rho_{so} = \frac{E_o^+(0)}{E_s(0)}, \tau_{so} = \frac{E_o^-(0)}{E_s(0)} \right\} \quad (48)$$

has to be modified. The other boundary matrix terms (T, R, $\boldsymbol{\tau}_{do}$, $\boldsymbol{\rho}_{do}$ and τ_{oo}) remain equivalent to SAIL++.

Moreover, $\boldsymbol{\rho}_{sd}$ is divided into two terms

$$\begin{aligned}
\boldsymbol{\rho}_{sd} &= \boldsymbol{\rho}_{sd}^1 + \boldsymbol{\rho}_{sd}^\infty, \\
\boldsymbol{\rho}_{sd}^1 &= \frac{E_+^0(0)}{E_s(0)}, \\
\boldsymbol{\rho}_{sd}^\infty &= \frac{E_+^\infty(0)}{E_s(0)}.
\end{aligned} \quad (49)$$

In the case of $x \in \{\tau_{ss}, \boldsymbol{\tau}_{sd}, \boldsymbol{\rho}_{sd}^\infty, \rho_{so}, \tau_{so}\}$ and according to Eqs. (47)

$$x = x^s + \sum_{n=0}^{\infty} (-1)^n \sum_{i=1}^{N} A_i^n (X_i^n x_{i,1}^n + Y_i^n x_{i,2}^n), \quad (50)$$

with x^s the value corresponding to the source E_s, and $\forall \{i,j,n\} \in \{1,\dots,N\} \times \{1,2\} \times \mathbb{N}, x_{i,j}^n$ the value corresponding to the source $E_{+,i,j}^{n,1}$. Based on Eqs. (43) (44)

$$\forall i \in \{1,\dots,N\}, \boldsymbol{\rho}_{sd}^1(i) = \sum_{n=0}^{\infty} (-1)^n A_i^n (X_i^n + Y_i^n \exp[-\boldsymbol{\kappa}_n(i)H]). \quad (51)$$

Note that τ_{ss}, the direct transmittance, does not change, it is equal to $\exp(-kH)$. Therefore, we have to derive only $\boldsymbol{\tau}_{sd}$, $\boldsymbol{\rho}_{sd}^\infty$, ρ_{so} and τ_{so}.

3.1.4 Sub-solution derivation

Here, we try to find the sub-solution scattering term expressions ($\boldsymbol{\tau}_{sd}$, $\boldsymbol{\rho}_{sd}^\infty$, ρ_{so} and τ_{so}) based on SAIL++ formalism and versus SAIL++ boundary matrix terms. To achieve it, the irradiance E_+^∞, E_- and radiances E_o have to be estimated. The latter terms have first to be estimated for each source among E_s and $\forall \{i,j,n\} \in \{1,\dots,N\} \times \{1,2\} \times \mathbb{N}, E_{-,i,j}^n$ and second combined using Eq. (47).

3.1.4.1 Source E_s

E_-^s, $E_+^{\infty,s}$, $E_o^{+,s}$ and $E_o^{-,s}$ verify

$$\frac{\mathrm{d}}{\mathrm{d}z} \begin{pmatrix} E_s \\ E_-^s \\ E_+^{\infty,s} \\ E_o^{+,s} \\ E_o^{-,s} \end{pmatrix} = \begin{pmatrix} k & 0 & 0 & 0 & 0 \\ -\mathbf{s}' & \mathbf{A} & -\mathbf{B} & 0 & 0 \\ 0 & \mathbf{B} & -\mathbf{A} & 0 & 0 \\ w & \mathbf{v} & \mathbf{v}' & -K & 0 \\ -w' & -\mathbf{v}' & -\mathbf{v} & 0 & K \end{pmatrix} \begin{pmatrix} E_s \\ E_-^s \\ E_+^{\infty,s} \\ E_o^{+,s} \\ E_o^{-,s} \end{pmatrix}, \quad (52)$$

Thus based on Eq. (88) notation, it follows

$$\begin{aligned}
\boldsymbol{\tau}_{sd}^s &= \boldsymbol{\tau}_{sd}^{++}(k,\mathbf{s}',0), \\
\boldsymbol{\rho}_{sd}^{s,\infty} &= \boldsymbol{\rho}_{sd}^{++}(k,\mathbf{s}',0), \\
\rho_{so}^s &= \rho_{so}^{HS,++}(k,\mathbf{s}',0,w), \\
\tau_{so}^s &= \tau_{so}^{++}(k,\mathbf{s}',0,w).
\end{aligned} \quad (53)$$

3.1.4.2 Source $E_{+,i,1}^{1,n}$

As for E_s [cf. Eq. (53)], it is straightforward to show that

$$
\begin{aligned}
\boldsymbol{\tau}_{sd,i,1}^{n} &= \boldsymbol{\tau}_{sd}^{++}(k,\mathbf{s}_{i,n},\mathbf{s}_{i,n}'), \\
\boldsymbol{\rho}_{sd,i,1}^{n,\infty} &= \boldsymbol{\rho}_{sd}^{++}(k,\mathbf{s}_{i,n},\mathbf{s}_{i,n}'), \\
\rho_{so,i,1}^{n} &= \rho_{so}^{++}(k,\mathbf{s}_{i,n},\mathbf{s}_{i,n}',w_{i,n}'), \\
\tau_{so,i,1}^{n} &= \tau_{so}^{++}(k,\mathbf{s}_{i,n},\mathbf{s}_{i,n}',w_{i,n}').
\end{aligned}
\tag{54}
$$

3.1.4.3 Source $E_{+,i,2}^{1,n}$

As for E_s [cf. Eq. (53)], it is straightforward to show that

$$
\begin{aligned}
\boldsymbol{\tau}_{sd,i,2}^{n} &= \boldsymbol{\rho}_{sd}^{++}(\boldsymbol{\kappa}_n(i),\mathbf{s}_{i,n}',\mathbf{s}_{i,n}), \\
\boldsymbol{\rho}_{sd,i,2}^{n,\infty} &= \boldsymbol{\tau}_{sd}^{++}(\boldsymbol{\kappa}_n(i),\mathbf{s}_{i,n}',\mathbf{s}_{i,n}), \\
\rho_{so,i,2}^{n} &= \tau_{so}^{++}(\boldsymbol{\kappa}_n(i),\mathbf{s}_{i,n}',\mathbf{s}_{i,n},w_{i,n}'), \\
\tau_{so,i,2}^{n} &= \rho_{so}^{++}(\boldsymbol{\kappa}_n(i),\mathbf{s}_{i,n}',\mathbf{s}_{i,n},w_{i,n}').
\end{aligned}
\tag{55}
$$

Finally, according to Eqs. (50) (53) (54) (55)

$$
\begin{aligned}
\boldsymbol{\tau}_{sd} &= \boldsymbol{\tau}_{sd}^{++}(k,\mathbf{s}',0) + \sum_{n=0}^{\infty}(-1)^n\sum_{i=1}^{N}A_i^n\big(X_i^n\boldsymbol{\tau}_{sd}^{++}(k,\mathbf{s}_{i,n},\mathbf{s}_{i,n}') + Y_i^n\boldsymbol{\rho}_{sd}^{++}(\boldsymbol{\kappa}_n(i),\mathbf{s}_{i,n}',\mathbf{s}_{i,n})\big), \\
\boldsymbol{\rho}_{sd}^{\infty} &= \boldsymbol{\rho}_{sd}^{++}(k,\mathbf{s}',0) + \sum_{n=0}^{\infty}(-1)^n\sum_{i=1}^{N}A_i^n\big(X_i^n\boldsymbol{\rho}_{sd}^{++}(k,\mathbf{s}_{i,n},\mathbf{s}_{i,n}') + Y_i^n\boldsymbol{\tau}_{sd}^{++}(\boldsymbol{\kappa}_n(i),\mathbf{s}_{i,n}',\mathbf{s}_{i,n})\big),
\end{aligned}
\tag{56}
$$

$$
\begin{aligned}
x_{so} &= \rho_{so}^{HS,++}(k,\mathbf{s}',0,w) + \sum_{n=0}^{\infty}(-1)^n\sum_{i=1}^{N} \quad A_i^n\big(X_i^n\rho_{so}^{++}(k,\mathbf{s}_{i,n},\mathbf{s}_{i,n}',w_{i,n}') + \\
& \qquad\qquad\qquad\qquad\qquad\qquad\qquad Y_i^n\tau_{so}^{++}(\boldsymbol{\kappa}_n(i),\mathbf{s}_{i,n}',\mathbf{s}_{i,n},w_{i,n})\big), \\
\tau_{so} &= \tau_{so}^{++}(k,\mathbf{s}',0,w) + \sum_{n=0}^{\infty}(-1)^n\sum_{i=1}^{N} \quad A_i^n\big(X_i^n\tau_{so}^{++}(k,\mathbf{s}_{i,n},\mathbf{s}_{i,n}',w_{i,n}') + \\
& \qquad\qquad\qquad\qquad\qquad\qquad\qquad Y_i^n\rho_{so}^{++}(\boldsymbol{\kappa}_n(i),\mathbf{s}_{i,n}',\mathbf{s}_{i,n},w_{i,n})\big).
\end{aligned}
\tag{57}
$$

3.2 Concatenation vegetation layer and soil background

Similarly to vegetation, one can define the directional-hemispherical reflectance ($\boldsymbol{r}_{sd}$), hemispherical-directional reflectance ($\boldsymbol{r}_{do}$) and hemispherical-hemispherical reflectance ($\boldsymbol{R}_{dd}$) fore soil which are two vectors and a matrix, respectively.

Based on Adding principle (Van de Hulst, 1980), Verhoef (1998) defines the bidirectional reflectance of the couple soil+vegetation (ρ_{so}^t) as

$$
\rho_{so}^{t} = \rho_{so} + \tau_{oo}r_{so}\tau_{ss} + (\tau_{oo}\boldsymbol{r}_{do}^{T} + \boldsymbol{\tau}_{do}^{T}\boldsymbol{R}_{dd})(1 - \mathrm{R}\boldsymbol{R}_{dd})^{-1}\boldsymbol{\tau}_{sd} + (\boldsymbol{\tau}_{do}^{T} + \tau_{oo}\boldsymbol{r}_{do}^{T}\mathrm{R})(I - \boldsymbol{R}_{dd}\mathrm{R})^{-1}\boldsymbol{r}_{sd}\tau_{ss},
\tag{58}
$$

with I the identity matrix.

Inspired from AddingSD (e.g. Kallel et al., 2008, p. 3647), we propose the following transformation of Eq. (58)

$$
\rho_{so}^{t} = \rho_{so} + \overbrace{\tau_{oo}r_{so}\tau_{ss}}^{r_{sso}} + \overbrace{\boldsymbol{\tau}_{do}^{T}\boldsymbol{r}_{sd}\tau_{ss}}^{r_{sdo}} + (\boldsymbol{\tau}_{do}^{T}\boldsymbol{R}_{dd} + \tau_{oo}\boldsymbol{r}_{do}^{T})(I - \mathrm{R}\boldsymbol{R}_{dd})^{-1}(\overbrace{\mathrm{R}\boldsymbol{r}_{sd}\tau_{ss} + \boldsymbol{\tau}_{sd}}^{\boldsymbol{\tau}_{sdd}}).
\tag{59}
$$

As rigourously explained in (Kallel et al., 2008), to pass from a turbid to a discrete case and take into account the hot spot effect as well as maintain energy conservation, we have to modify the expression of r_{sso}, r_{sdo} and $\boldsymbol{\tau}_{sdd}$ by considering the actual local vegetation density:

- r_{sso} corresponds to the flux passing through the vegetation layer from top to bottom without collision, scattered by the soil and reaching the top of the vegetation without other collisions. For this flux, the classical hot spot effect should be computed as

$$r_{sso} = r_{so} \exp\left[-(k+K)H + \frac{\sqrt{kK}}{b}[1 - \exp(-bH)] \right]; \qquad (60)$$

- $\boldsymbol{\tau}_{sdd}$ corresponds to the flux passing through the vegetation layer from top to bottom without collisions, scattered by the soil, colliding with the vegetation and reaching the soil again.

- r_{sdo} corresponds to the flux passing through the vegetation layer from top to bottom without collisions, scattered by the soil and reaching the top of the vegetation after multiple collisions.

Using the same principle that for E_+^1 scattering derivation, it is straightforward to show that

$$
\begin{aligned}
\boldsymbol{\tau}_{sdd} &= \exp(-kH) \sum_{n=0}^{\infty} (-1)^n \sum_{i=1}^{N} A_i^n \mathbf{a}(i) \boldsymbol{\rho}_{sd}^{++}(\kappa_n(i), \mathbf{s}'_{i,n}, \mathbf{s}_{i,n}), \\
r_{sdo} &= \exp(-kH) \sum_{n=0}^{\infty} (-1)^n \sum_{i=1}^{N} A_i^n \mathbf{a}(i) \tau_{so}^{++}(\kappa_n(i), \mathbf{s}'_{i,n}, \mathbf{s}_{i,n}, w_{i,n}).
\end{aligned}
\qquad (61)
$$

4. Virtual flux decomposition validation

This section is dedicated to the validation of our virtual flux decomposition. The corresponding will be called the Flux Decomposition Model (FDM). First, model convergence and running time are presented. Second, energy conservation is shown. Third, a comparison between our approach and SAIL/SAIL++ models is presented. Finally, our model is compared to the 3-D models of the RAMI 2 database assumed 'most credible'.

Among the most commonly used models to describe the distribution of leaf zenithal angles is the method assuming an elliptic leaf distribution where the distribution is parameterized by the mean leaf inclination angle, ALA, ranging between 0 and $90°$ (Campbell, 1990). We will use this distribution in our model simulations. Note that small ALA values correspond to planophile distributions, high values to erectophile distributions, and medium values to extremophile distributions. Moreover, to be compatible with RAMI database simulations, Bunnik's [1978] parametrization will be used in the fourth subsection.

Since FDM is equivalent to SAIL++ in the turbid case. In this paper, we will deal only with the discrete case.

4.1 Running time

Among the strengths of our model is its low running time. The decomposition of L_+^1 into virtual sub-fluxes allowed the use of SAIL++ formalism to solve the RT problem.

Although, according to Eqs. (56) (57) (61), an infinite number of SAIL++ simulations is needed to derive the reflectance, only few first ranked terms are used to achieve accurate results. The sum is provided by Taylor series decomposition. Next, we will present a study on the accuracy of the approximation.

Here, we opt to use fluxes (E_+^∞ in our case) and the corresponding hemispherical scattering (ρ_{sd}^∞) term rather than radiances E_o^+ or E_o^-. For energy conservation, it is more significant to deal with fluxes than their densities.

Recall that

$$
\begin{aligned}
E_+^\infty &= E_+^{\infty,s} + \sum_{n=0}^{\infty} (-1)^n \sum_{i=1}^{N} A_i^n (X_i^n E_{+,i,j}^{\infty,n} + Y_i^n E_{+,i,j}^{\infty,n}) = E_+^{\infty,s} + \sum_{n=0}^{\infty} (-1)^n \sum_{i=1}^{N} A_i^n E_{+,i}^{\infty,n}, \\
&= E_+^{\infty,s} + \sum_{i=1}^{N} \sum_{n=0}^{\infty} (-1)^n A_i^n E_{+,i}^{\infty,n},
\end{aligned}
\tag{62}
$$

where $E_{+,i}^{\infty,n}$ is the high order diffuse flux created by $E_{+,i}^{1,n}$. Now, according to Eq. (22), $E_{+,i}^{1,n}$ is created by E_S scattering. Then, due to the energy conservation law

$$
\forall (z,i) \in [-H,0] \times \{1,\ldots,N\}, ||E_{+,i}^{\infty,n}(z)|| \leq E_s(0),
\tag{63}
$$

where $||.||$ of a given discrete flux over a hemisphere is the sum of the sub-fluxes' values in each segment. It corresponds to the integrate radiance distribution over the hemisphere.

Let us assume that, $\forall i \in \{1,\ldots,N\}$, the series $\sum_{n=0}^{\infty} (-1)^n A_i^n E_{+,i}^{\infty,n}$ is truncated to the order u_i. Let us define a vector $\boldsymbol{u}$ by

$$
\boldsymbol{u} = [u_1,\ldots,u_N],
\tag{64}
$$

and the corresponding flux $E_+^{\infty,\boldsymbol{u}}$

$$
E_+^{\infty,\boldsymbol{u}} = E_+^{\infty,s} + \sum_{i=1}^{N} \sum_{n=0}^{u_i} (-1)^n A_i^n E_{+,i}^{\infty,n},
\tag{65}
$$

then

$$
\begin{aligned}
||E_+^\infty - E_+^{\infty,\boldsymbol{u}}|| &= ||\sum_{i=1}^{N} \sum_{n=u_i+1}^{\infty} (-1)^n A_i^n E_{+,i}^{\infty,n}|| \leq \sum_{i=1}^{N} \sum_{n=u_i+1}^{\infty} A_i^n ||E_{+,i}^{\infty,n}|| \leq \sum_{i=1}^{N} \sum_{n=u_i+1}^{\infty} A_i^n E_s(0), \\
&\leq E_s(0) \sum_{i=1}^{N} \exp\left[\frac{\sqrt{k\kappa(i)}}{\boldsymbol{b}(i)}\right] \sum_{n=u_i+1}^{\infty} \frac{(k\kappa(i))^{n/2}}{n! \boldsymbol{b}(i)^n}, \\
&\leq E_s(0) \sum_{i=1}^{N} \exp\left[\frac{\sqrt{k\kappa(i)}}{\boldsymbol{b}(i)}\right] \frac{(k\kappa(i))^{(u_i+1)/2}}{(u_i+1)! \boldsymbol{b}(i)^{u_i+1}} \sum_{n=0}^{\infty} \frac{(k\kappa(i))^{n/2}(u_i+1)!}{(n+u_i+1)! \boldsymbol{b}(i)^n}, \\
&\leq E_s(0) \sum_{i=1}^{N} \exp\left[\frac{\sqrt{k\kappa(i)}}{\boldsymbol{b}(i)}\right] \frac{(k\kappa(i))^{(u_i+1)/2}}{(u_i+1)! \boldsymbol{b}(i)^{u_i+1}} \sum_{n=0}^{\infty} \frac{(k\kappa(i))^{n/2}}{n! \boldsymbol{b}(i)^n}, \\
&\leq E_s(0) \sum_{i=1}^{N} \underbrace{\exp\left[\frac{\sqrt{k\kappa(i)}}{\boldsymbol{b}(i)}\right] A_i^{u_i+1}}_{B_i^{u_i+1}}.
\end{aligned}
\tag{66}
$$

It is clear that, $\lim_{u_i \to +\infty} B_i^{u_i+1} = 0$, then

$$
\lim_{u_1 \to +\infty} \lim_{u_2 \to +\infty} \ldots \lim_{u_N \to +\infty} ||E_+^\infty - E_+^{\infty,\boldsymbol{u}}|| = 0.
\tag{67}
$$

Thank You for previewing this eBook

You can read the full version of this eBook in different formats:

- ➢ HTML (Free /Available to everyone)

- ➢ PDF / TXT (Available to V.I.P. members. Free Standard members can access up to 5 PDF/TXT eBooks per month each month)

- ➢ Epub & Mobipocket (Exclusive to V.I.P. members)

To download this full book, simply select the format you desire below